

Nd isotopic compositions of the Tethyan Himalayan Sequence in southeastern Tibet

DAI JinGen¹, YIN An^{1,2†}, LIU WenCan¹ & WANG ChengShan¹

¹ State Key Laboratory of Geological Processes and Mineral Resources, Research Center for Tibetan Plateau Geology and School of Geosciences, China University of Geosciences, Beijing 100083, China;

² Department of Earth and Space Sciences and Institute of Geophysics and Planetary Physics, University of California, Los Angeles, CA 90095-1567, USA

The Himalayan orogen consists of three major lithologic units that are separated by two major north-dipping faults: the Lesser Himalayan Sequence (LHS) below the Main Central Thrust (MCT), the Greater Himalayan Crystalline Complex (GHC) above the MCT, and the Tethyan Himalayan Sequence (THS) juxtaposed by the South Tibet Detachment fault (STD) over the GHC. Due to widespread metamorphism and intense deformation, differentiating the above three lithologic units is often difficult. This problem has been overcome by the use of Sm-Nd isotopic analysis. The previous studies suggested that the LHS can be clearly distinguished from the GHC and THS by their Nd isotope compositions. However, the lack of detailed and systematic Sm-Nd isotopic studies of the THS across the Himalaya in general has made differentiation of this unit from the nearby GHC impossible, as the two appear to share overlapping Nd compositions and model ages. To address this problem, we systematically sampled and analyzed Nd isotopes of the THS in southeastern Tibet directly north of Bhutan. Our study identifies two distinctive fields in a $\epsilon_{\text{Nd}}-T_{\text{DM}}$ plot. The first is defined by the $\epsilon_{\text{Nd}}(210 \text{ Ma})$ values of -3.45 to -7.34 and T_{DM} values of 1.15 to 1.29 Ga from a Late Triassic turbidite sequence, which are broadly similar to those obtained from the Lhasa block. The second field is derived from the Early Cretaceous meta-sedimentary rocks with $\epsilon_{\text{Nd}}(130 \text{ Ma})$ values from -15.24 to -16.61 and T_{DM} values from 1.63 to 2.00 Ga; these values are similar to those obtained from the Greater Himalayan Crystalline Complex in Bhutan directly south of our sampling traverse, which has $\epsilon_{\text{Nd}}(130 \text{ Ma})$ values of -10.89 to -16.32 and Nd model ages (T_{DM}) of 1.73 to 2.20 Ga. From the above observations, we suggest that the Late Triassic strata of the southeast Tibetan THS were derived from the Lhasa block in the north, while the Early Cretaceous strata of the THS were derived from a source similar to the High Himalayan Crystalline Complex or Indian craton in the south. Our interpretation is consistent with the existing palaeocurrent data and provenance analysis of the Late Triassic strata in southeastern Tibet, which indicate the sediments derived from a northern source. Thus, we suggest that the Lhasa terrane and the Indian craton were close to one another in the Late Triassic and were separated by a rift valley across which a large submarine fan was transported southward and deposited on the future northern margin of the Indian continent.

Himalayan orogen, Sm-Nd isotopic systematics, Greater Himalayan Crystalline Complex, Tethyan Himalaya Sequence, Lhasa terrane, Indian craton

Received March 13, 2008; accepted June 5, 2008

doi: 10.1007/s11430-008-0103-7

†Corresponding author (email: yin@ess.ucla.edu)

Supported by China University of Geosciences (Beijing) and a Changjiang Fellowship from the Chinese Ministry of Education awarded to Yin An

1 Introduction

The Himalayan orogen consists of three lithologic units that are stacked over one another by orogen-scale, north-dipping faults: the Lesser Himalayan Sequence (LHS) at the lowest structural level between the Main Boundary Thrust (MBT) below and the Main Central Thrust (MCT) above, the Greater Himalayan Crystalline Complex (GHC) in the middle structural level between the MCT below and the South Tibet Detachment fault (STD) above, and the Tethyan Himalayan Sequence (THS) at the highest structural level above the STD (Figure 1)^[1–4]. The LHS consists of a Mesoproterozoic to Cambrian sedimentary sequence and is considered to be in depositional contact on top of the Archean and early Proterozoic Indian crystalline basement^[5,6]. The GHC is a high-grade metamorphic complex containing meta-sedimentary sequences that are intruded by deformed granitoids with ages of 487–550 Ma^[7]. However, an orthogneiss with a U-Pb zircon age of 825 Ma intrudes a quartzite of the GHC in Bhutan^[8], implying that at least some portions of the GHC metasediments are older than 825 Ma. Although dominant Himalayan metamorphism event occurred in the Cenozoic, the GHC has also experienced metamorphism at garnet grade at around 500 Ma, possibly related to collision of India with an exotic terrane in the Cambrian-Ordovician^[9–12]. The exotic terrane hypothesis for the origin of the GHC has been disputed by Myrow et al.^[13] who suggested that the GHC was part of northern Indian margin despite the noted early Paleozoic deformation. The THS records continuous marine sedimentation from the Cambrian to the Eocene on the northern Indian margin^[6]. Marine sedimentation from Cambrian to Permian time mostly occurred in a cratonal setting, although Carboniferous rifting locally disrupted this simple sedimentation pattern^[14]. Triassic to Early Jurassic time marks the initiation of a major rifting event on the northern Indian margin, as expressed by basaltic eruption and deposition of a thick carbonate and siliciclastic sequence^[3,15,16]. This rifting has been related to the separation of the Lhasa block from India^[3,17,18].

Due to widespread Cenozoic metamorphism and deformation across the Himalayan orogen, differentiating the major Himalayan units has proven difficult in the field. This has led to debates on the exact locations of major structures such as the MCT and STD in some

parts of the Himalayan orogen^[5,19–22]. For this reason, some workers used Nd isotopic compositions to differentiate major Himalayan units^[8,11,13,23–26]. The existing Nd and Sr isotopic data suggest Nd model ages of the THS between 1.14 and 2.31 Ga, $\epsilon_{\text{Nd}}(0)$ values between –20.05 and –6.16, and $^{87}\text{Sr}/^{86}\text{Sr}$ initial ratios between 0.705 and 0.750^[24–29]. The GHC and THS have similar Nd composition with $\epsilon_{\text{Nd}}(0)$ between –19.06 and –6.16^[8,11,12,22,23,25–27,30–32]. The LHS typically has $\epsilon_{\text{Nd}}(0)$ values between –32.26 and –15.92, and T_{DM} values from 1.84 Ga to 2.84 Ga, indicating a much older crust as its source^[8,11,22,23,25,26,28,32].

The major problems with the existing chemo-stratigraphy of the Himalayan units are that (1) it has focused almost exclusively in the western and central Himalaya with only a sparse coverage of the eastern Himalaya, and (2) the number of samples analyzed from the THS is significantly less than those from the GHC and LHS units (see Yin^[4] for a review of this problem). The latter issue makes it ambiguous whether the similar Nd isotopic composition of the GHC and THS is an artifact of incomplete sampling of THS strata.

To address the above issue we conducted systematic sampling of the THS in the eastern Himalayan orogen in southeast Tibet. Our work indicates significant internal variation of Nd isotope variations within the THS between the Late Triassic and Early Cretaceous strata. The former exhibits Nd isotopic compositions similar to those from the Tibetan terranes whereas the latter has Nd compositions similar to the GHC. The similarity in the Nd isotope values between the Triassic strata in the THS on the northern Indian margin and the Tibetan terranes, along with early work indicating that the Triassic sediments in southeast Tibet were transported from a northern source, supports the early proposal that the Lhasa terrane and the Indian craton were both parts of the Gondwana; they were separated in the early Jurassic during the opening of the Neo-Tethys^[3,15,16]. This geologic link suggests that Nd isotopic composition alone cannot be used as the sole criterion to differentiate Tibetan terranes from the Indian lithologic units^[33,34].

2 Regional geology

The eastern Himalayan orogen lies between longitude 88°E and 98°E and is bounded by the Indus-Tsangpo suture in the north and the Himalayan foreland basin in

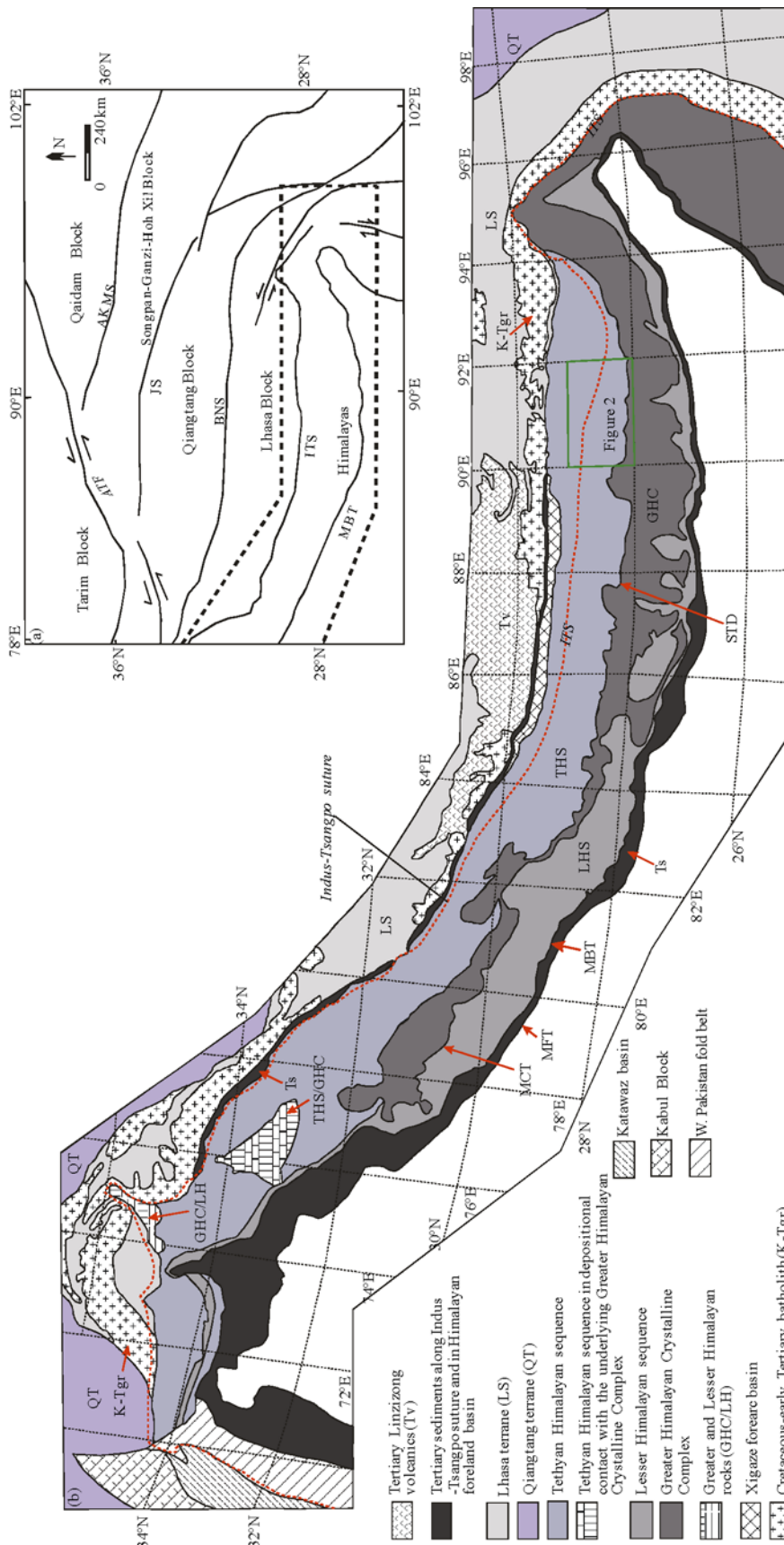


Figure 1 (a) Simplified tectonic framework of the Tibetan-Himalayan orogen (modified from Yin and Harrison^[18]); (b) regional geologic map of the Himalayan orogen (adapted from Yin^[4]). Major lithologic units: Ts, Tertiary sediments; THS/GHC, Lesser Himalayan Sequence; LHS, Lesser Himalayan Sequence; THS/GHC, unmetamorphosed (with respect to Cenozoic deformation) Tethyan and Greater Himalayan Sequences; GHC, Greater Himalayan Crystalline Complex. Major faults: MBT, Main Boundary Thrust; MCT, Main Central Thrust; MFT, Main Frontal Thrust; STD, South Tibet Detachment. Major sutures: BNS, Bangong-Nujiang suture; JS, Jinsha suture; AKMS, Aymaqin-Kunlun-Mutztagh suture.

the south (Figure 1). The three major Himalayan units, LHS, GHC, and THS are separated by the MCT and the STD^[2,35–38]. The geology of the high-grade GHC above the MCT and the LHS below the thrust is best studied in Bhutan and around the eastern Himalayan syntaxis. In Bhutan, the LHS consists of garnet-bearing schist, quartzite, phyllite, and granitic gneisses whereas the GHC is composed of paragneiss, orthogneiss, migmatite, and Tertiary leucogranite^[39,40]. The LHS schist unit experienced peak metamorphism at 650–675 °C and 9.1×10^8 – 1.3×10^9 Pa at 18–22 Ma^[41], whereas the granitic gneiss units have yielded a Rb-Sr age of ~1.1 Ga^[40] and a U-Pb zircon age of ~1.76 Ga^[41]. The LHS also contains a 1.8–1.9 Ga meta-rhyolite and an arenite unit with U-Pb detrital zircon ages between 1.8 and 2.5 Ga^[8]. Kyanite-bearing migmatites in the GHC experienced a peak *P-T* condition of ~750–800 °C and 1.0×10^9 – 1.4×10^9 Pa at ~18 Ma, followed by retrograde metamorphism under a condition of 500–600 °C and 5.0×10^8 Pa; the latter was associated with intrusion of 13 Ma leucogranite and a 14–11 Ma cooling event in the MCT zone^[41,42]. A quartzite unit yielding U-Pb detrital zircon ages of 980–1820 Ma in the GHC is intruded by an 825 Ma orthogneiss^[8]. The GHC and LHS appear to have distinctive Nd isotope compositions, with the corresponding Nd model ages T_{DM} ranging from 1.73 to 2.20 Ga for the LHS and 2.46 to 2.61 Ga for the GHC^[8]. The eastern Himalayan syntaxis consists of metamorphic rocks that record a peak condition of ~800 °C and $\sim 1.5 \times 10^9$ Pa^[43]. The high-grade rocks experienced magmatism at 400–500, 120, 40–70, 18–25, and 3–10 Ma^[44]. Exceptionally young (<10 Ma) zircon ages and ⁴⁰Ar/³⁹Ar muscovite ages are clustered at the core of the syntaxis, which may be a result of focused exhumation^[45].

Our study area is located on the north slope of the Himalayan Range in southeast Tibet, between longitude 90°E and 92°E (Figure 2). In the north, the THS is bounded by the south-dipping Oligocene-Miocene Renbu-Zedong Thrust (RZT), which places the THS (mainly Triassic flysch complex) over the Cretaceous-Early Tertiary Gangdese batholith^[46–49]. In the south, the THS is bounded by the north-dipping STD. The THS between the RZT and STD is internally divided by two north-dipping thrusts (Figure 2). The northern thrust places Late Triassic strata over Jurassic and Early Cretaceous sediments, and the southern thrust

places Jurassic strata over Cretaceous strata (Figure 2). Although major lithologic units in the study area are Late Triassic to Cretaceous in age, Late Proterozoic and Early Paleozoic metasedimentary rocks are also exposed around the Yala Xianbo gneiss dome in the easternmost part of the study area, all of which had experienced high-grade metamorphism in the Cenozoic (Figure 2)^[50]. The THS strata in our study area experienced isoclinally folding and the bedding in many places is completely transposed by axial cleavage. Although the age of the THS units generally decreases southward, their metamorphic grade increases steadily to the south, reaching to the garnet grade directly above the STD near the China-Bhutan border. The Triassic strata against the suture zone in the north are mostly in the lower greenschist facies, containing chlorite. To the south near the STD Cretaceous marine strata are metamorphosed to become schist and meta-greywacke, containing biotite, muscovite, and locally garnet. The high-grade Cretaceous metamorphic rocks are also intruded by Tertiary leucogranites directly above the STD (Figure 2). Due to intense deformation and metamorphism, the ages of Triassic and Cretaceous strata are not well constrained; their age estimates are established from lithostratigraphic correlations with the better dated Late Triassic strata by fossils in the regions directly to the west of our study area^[51]. Some of the Triassic units in our area have been reinterpreted to be Cretaceous owing to the discovery of ammonoids^[50,52,53].

3 Nd isotope analysis

3.1 Samples

A total of 10 samples were collected from 7 locations for Nd isotope analysis and the results are summarized in Table 1 (Figure 2). Among them four samples were collected from the Late Triassic Langjiexue Group and six samples were collected from Early Cretaceous Lhakang Formation (Figure 2). The Langjiexue Group is dominated by turbidite sequences comprising mudstone, siltstone, and sandstone. Its lithology, provenance, sedimentary structures, and depositional setting were examined in detail by Li et al.^[54–56]. Sedimentary structures such as tool marks and cross-bedding relationships suggest that the paleocurrent directions during the deposition of the Late Triassic strata were mainly southward, with minor components to the southwest and south-

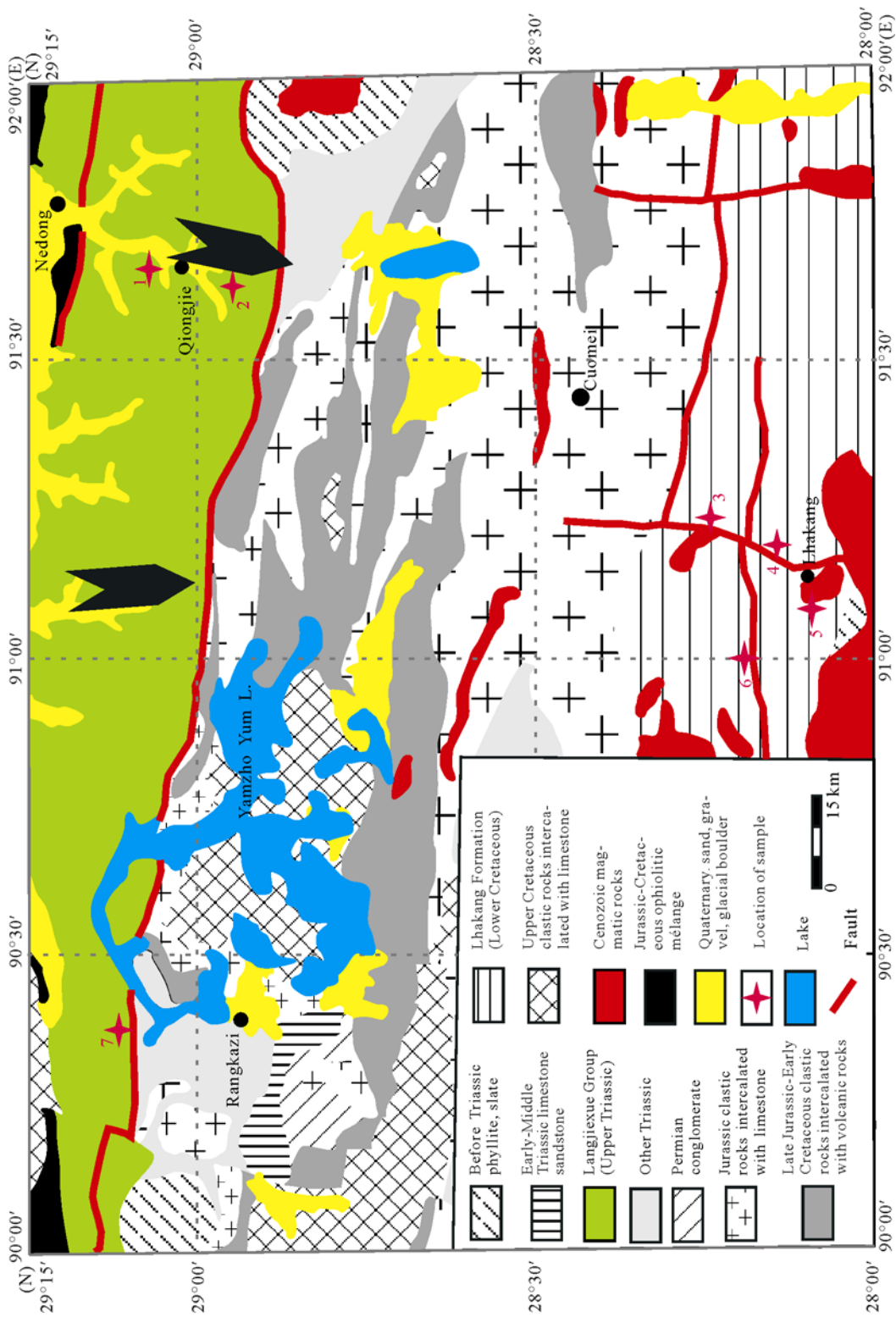


Figure 2 Geologic map of the study area in southeastern Tibet (modified from ref. [50]). Sample locations of this study are also indicated. Samples 1, 2, and 7 were collected from the Upper Triassic Langjiexue Group, while samples 3, 4, 5, and 6 were collected from the Lower Cretaceous Lhakang Formation. The arrows in the northeastern part of the map represent paleocurrent directions reconstructed for the Late Triassic Langjiexue Group by Li et al. [54].

east^[54]. Basin analysis of the Triassic strata led Li et al.^[55] to conclude that the sediments were deposited in a south-flowing submarine fan system that had migrated southward during their build-ups. Sandstone composition analysis of the Triassic turbidite suggests it to have been derived from a recycled orogen, with lithic fragments dominated by sedimentary and metamorphic detritus^[56]. Additionally, trace element analysis indicates that the source region of the Triassic strata consists of a continental arc and a passive continental margin^[56]. Li et al.^[56] speculated that the northern source region of the Triassic fan system was the Lhasa block before the birth of the Early Jurassic Neo-Tethys when it was finally separated from India during the breakup of the Gondwana. Unlike the Triassic strata in southwest Tibet, sedimentology and depositional settings of the Cretaceous strata have not been examined in detail. This is in part due to the fact that the unit has experienced much higher grade metamorphism and stronger contractional deformation, which have eliminated most original sedimentary structures due to transposition of original bedding to metamorphic foliation. Nevertheless, the work by Xia et al.^[52] and Zhong et al.^[53] suggests that the Lhakang Formation comprises sandstone, siltstone, slate, and micritic limestone that have all undergone biotite to garnet grade metamorphism. The above study also indicates that the unit was deposited in a lagoonal environment along the northern margin of the Indian continent.

3.2 Method

Sm-Nd isotopic compositions were determined on bulk rocks which were powdered to less than 200 mesh. Sm-Nd isotopic analyses were carried out on 120–150 mg of the bulk rock powders to which a ¹⁴⁹Sm-¹⁵⁰Nd spike had been added. The samples were dissolved by using a mixture of HF-HClO₄ in Teflon bombs at 100–120°C for seven days. The samples were then dried at 180°C. After several rounds of HCl treatments, Sm and Nd isotopes were separated and measured following standard procedures outlined by Hegner et al.^[57]. Sm-Nd was separated from rare-earth elements on quartz columns using 1 mL Teflon powder coated with HDEHP, di(2-ethylhexyl) orthophosphoric acid, as the cation exchange medium. Sm-Nd isotopic compositions were measured by Finnigan MAT 262 Thermal Ionization Mass Spectrometer (TIMS) at the Laboratory for Radiogenic Isotope Geochemistry in the Institute of Geology and Geophysics, the Chinese Academy of Sciences

(Beijing). Sm-Nd were loaded as phosphate on pre-conditioned Re filaments and then measured in a Re double filament configuration. ¹⁴³Nd/¹⁴⁴Nd ratios are normalized to ¹⁴⁶Nd/¹⁴⁴Nd=0.7219 and Sm isotopic ratios to ¹⁴⁷Sm/¹⁵²Sm=0.56081. All errors quoted in Table 1 correspond to 2 sigma standard deviation from the mean. During the study the isotopic analyses of the Ames Nd standard yielded ¹⁴³Nd/¹⁴⁴Nd=0.512129±11 (2σ, n=5). The total procedural blanks were < 50 pg for Sm and Nd. Further details on the Sm-Nd analytical techniques are described by Chen et al.^[58,59].

3.3 Results

Results of Sm-Nd isotopic analysis of bulk rocks are summarized in Table 1. In general, samples from Triassic and Cretaceous strata have different Nd isotope compositions, with the former having much less negative $\epsilon_{Nd}(0)$ values (–5.42 to –9.76) and younger Nd model ages (1.15–1.29 Ga) than the latter with the $\epsilon_{Nd}(0)$ values from –16.74 to –18.00 and Nd model ages from 1.63 to 2.00 Ga. We describe our results in detail below.

Four samples were collected from the Late Triassic Langjiexue Group. Sample AY06-29-06-8A from sample site 1 is coarse-grained sandstone in the northernmost part of our sampling traverse (Figure 2). This sample has a $\epsilon_{Nd}(0)$ value of –8.63 and a $\epsilon_{Nd}(210 \text{ Ma})$ value of –6.27. Its Nd model age is 1.23 Ga calculated using the deleted mantle model of DePaolo^[60]. From the same sample location, we also analyzed a finer-grained siltstone sample (sample AY06-29-06-8B), which yields slightly less negative $\epsilon_{Nd}(0)$ (–8.15) and $\epsilon_{Nd}(210 \text{ Ma})$ (–5.75) values and a younger Nd model age (1.18 Ma) than the coarser grained sample from the same site (Table 1). Sample AY06-29-06-9A was collected at sample site 2 from the Late Triassic strata (Figure 2). This sample yields a $\epsilon_{Nd}(0)$ value of –9.76 and a $\epsilon_{Nd}(210 \text{ Ma})$ value of –7.34, with a Nd model age of 1.29 Ga. Sample AY07-03-06-1 is meta-greywacke from the Late Triassic strata at sample location 7 (Figure 2). It has a $\epsilon_{Nd}(0)$ value of –5.42 and a $\epsilon_{Nd}(210 \text{ Ma})$ value of –3.45, with a Nd model age of 1.15 Ga.

In contrast to Triassic samples, Cretaceous samples generally have much lower $\epsilon_{Nd}(0)$ values and much older Nd model ages (Table 1). Sample AY07-01-06-2 was collected from a slate unit at sample site 3 (Figure 2).

This sample yields a $\epsilon_{Nd}(0)$ value of –16.84 and a

Table 1 Sm-Nd isotopic data of siliciclastic rocks from southeastern Tibet

Sample No.	Location	Lithology	Sm (ppm)	Nd (ppm)	$^{147}\text{Sm}/^{144}\text{Nd}$	$^{143}\text{Nd}/^{144}\text{Nd}$	Error (2 σ)	$\varepsilon_{\text{Nd}}(0)^{\text{e}}$	$\varepsilon_{\text{Nd}}(t)^{\text{d}}$	T_{DM} (Ma) ^e	Age (Ma)
AY06-29-06-8A1 ^{a)}	28°58.279'N 91°39.571'E	coarse-gd ss ^{b)}	5.21	28.99	0.1087	0.512196	13	-8.63	-6.27	1230	210
AY06-29-06-8B1	28°58.279'N 91°39.571'E	siltstone	7.96	45.06	0.1068	0.512220	14	-8.15	-5.75	1175	210
AY06-29-06-9A2	28°56.997'N 91°38.927'E	fine-grained phyllite	8.89	50.53	0.1063	0.512138	14	-9.76	-7.34	1286	210
AY07-03-06-17	29°05.565'N 90°23.602'E	meta-greywacke	6.31	30.96	0.1232	0.512360	13	-5.42	-3.45	1152	210
AY07-01-06-23	28°15.604'N 91°13.699'E	slate	4.83	27.23	0.1072	0.511775	12	-16.84	-15.36	1815	130
AY07-01-06-5A4	28°10.404'N 91°14.165'E	meta-pelite	6.95	44.37	0.0947	0.511770	10	-16.93	-15.24	1630	130
AY07-01-06-5B4	28°10.404'N 91°14.165'E	quartz arenite	6.63	35.57	0.1128	0.511742	14	-17.47	-16.08	1965	130
AY07-02-06-45	28°07.270'N 91°05.805'E	phyllite	7.81	46.06	0.1025	0.512230	12	-7.95	-6.39	1117	130
AY07-02-06-6A6	28°13.144'N 91°00.510'E	sandy phyllite	6.26	33.64	0.1125	0.511715	13	-18.00	-16.61	2002	130
AY07-02-06-6B6	28°13.144'N 91°00.510'E	phyllite	10.94	61.92	0.1068	0.511780	14	-16.74	-15.25	1799	130

a) Sample numbers correspond to those shown in Figure 2. b) Coarse-grained sandstone. c) Calculated at the present. d) Calculated at assumed age according to the sedimentary age in order to get initial values. $\varepsilon_{\text{Nd}}(t) = \varepsilon_{\text{Nd}}(0) - f_{\text{Sm}/\text{Nd}} \times Q_{\text{Nd}} \times t$, $Q_{\text{Nd}} = \lambda \times (^{147}\text{Sm}/^{144}\text{Nd})_{\text{CHUR}}(0) / (^{143}\text{Nd}/^{144}\text{Nd})_{\text{CHUR}}(0) \times 10^4$, $f_{\text{Sm}/\text{Nd}} = (^{147}\text{Sm}/^{144}\text{Nd})_{\text{sample}}(0) / (^{147}\text{Sm}/^{144}\text{Nd})_{\text{CHUR}}(0) - 1$, $(^{143}\text{Nd}/^{144}\text{Nd})_{\text{CHUR}}(0) = 0.512638$, $(^{147}\text{Sm}/^{144}\text{Nd})_{\text{CHUR}}(0) = 0.1967$, the two values are the ratio of CHUR at present time, and normalized to $^{146}\text{Nd}/^{144}\text{Nd} = 0.7219$. And $Q_{\text{Nd}} = 25.09 \text{ Ga}^{-1}$, $\lambda = 6.54 \times 10^{-12} \text{ a}^{-1}$. e) T_{DM} is model age or crustal residence age, represents the age of crustal material separated from depleted mantle, T_{DM} were calculated by using the quadratic solution for depleted mantle evolution of DePaolo^[60], that is, $\varepsilon_{\text{Nd}}(T_{\text{DM}}) = 0.25T_{\text{DM}}^2 - 3T_{\text{DM}} + 8.5$, $\varepsilon_{\text{Nd}}(0) - f_{\text{Sm}/\text{Nd}} \times Q_{\text{Nd}} \times T_{\text{DM}} = 0.25T_{\text{DM}}^2 - 3T_{\text{DM}} + 8.5$.

$\varepsilon_{\text{Nd}}(130 \text{ Ma})$ value of -15.36 , with its Nd model age of 1.82 Ga. Sample AY07-01-06-5A is meta-pelite collected at sample location 4 (Figure 2). This sample yields a $\varepsilon_{\text{Nd}}(0)$ value of -16.93 and a $\varepsilon_{\text{Nd}}(130 \text{ Ma})$ value of -15.24 , with its Nd model age of 1.63 Ga. Sample AY07-01-06-5B is quartz arenite collected from the same location as sample AY07-01-06-5A (sample site 4 in Figure 2). This sample yields a $\varepsilon_{\text{Nd}}(0)$ value of -17.47 and a $\varepsilon_{\text{Nd}}(100 \text{ Ma})$ value of -16.08 , with its Nd model age of 1.97 Ga. Sample AY07-02-06-6A is sandy phyllite collected at sample location 6 (Figure 2). This sample yields a $\varepsilon_{\text{Nd}}(0)$ value of -18.00 and a $\varepsilon_{\text{Nd}}(130 \text{ Ma})$ value of -16.61 , with its Nd model age of 2.00 Ga. From the same location, a finer-grained phyllite sample (sample AY07-02-06-6B) was also analyzed. This sample yields less negative $\varepsilon_{\text{Nd}}(0)$ (-16.74) and $\varepsilon_{\text{Nd}}(130 \text{ Ma})$ (-15.25) values than the coarse grained sample from the same site.

Although the above Cretaceous samples all yield significantly more negative $\varepsilon_{\text{Nd}}(0)$ values and older Nd model ages, one Cretaceous sample (sample AY07-02-06-4) collected from sample site 5 near a Tertiary leucogranite yields a Nd composition that is drastically different from the rest of the Cretaceous Nd isotope compositions but similar to the values obtained

from our Triassic samples (Figure 2, Table 1). Specifically, this sample yields a $\varepsilon_{\text{Nd}}(0)$ value of -7.95 and a $\varepsilon_{\text{Nd}}(130 \text{ Ma})$ value of -6.39 , with its Nd model age of 1.12 Ga. There are at least three possible explanations for this anomalous Nd isotopic composition. First, the age assignment of the unit is in error. We note that the Cretaceous unit south of the southern thrust in the study area, as mentioned above, was originally assigned with a Triassic age in Liu^[61]. However, recent discovery of Cretaceous fossils in a sequence with a similar lithology in an area to the west led Pan et al.^[50] to reinterpret the entire fault-bounded panel to be Cretaceous in age. In the field, we observed that the lithology of the Cretaceous unit of Pan et al.^[50] in places is similar to their Late Triassic strata except that the former has experienced a higher-grade metamorphism. We also noticed that the Cretaceous unit of Pan et al.^[50], as shown in Figure 2, is isoclinally folded and its bedding is mostly transposed by metamorphic foliation and slaty cleavage. As a result, it is possible that the folded sequence contains fragments of Triassic strata such as in the core of an anticline. The second possibility is that the Cretaceous strata record a drastic change in sedimentary sources, some being similar to those for the Triassic rocks. The third possibility is that sample AY07-02-06-4

may contain young volcanic ashes, which were ejected from volcanic centers along the northeastern margin of India during its separation from Australia and Antarctica in the Early Cretaceous^[62,63]. Young felsic volcanic ashes may be responsible for the rise of the $^{147}\text{Sm}/^{144}\text{Nd}$ ratio. Interestingly, Robinson et al.^[26] have reported similar ϵ_{Nd} and T_{DM} values for one of their samples from the Cretaceous Chukh Formation in the uppermost part of the THS in central Nepal; that sample has $\epsilon_{\text{Nd}}(100 \text{ Ma}) = -5.15$ and $T_{\text{DM}} = 1.31 \text{ Ga}$, similar to our results. Differentiating the above possibilities requires much more careful and systematic structural, stratigraphic, and isotopic analysis of the Cretaceous strata mapped by Pan et al.^[50] between the STD and the southern thrust in the area. We do not consider the emplacement of the nearby Tertiary leucogranite to have had any effect on the Nd isotopic composition of this anomalous sample. The Himalayan leucogranites typically have Nd compositions and model ages similar to those for the GHC, which are very similar to the values we obtained for all but one of the Cretaceous samples^[11] (Figure 3).

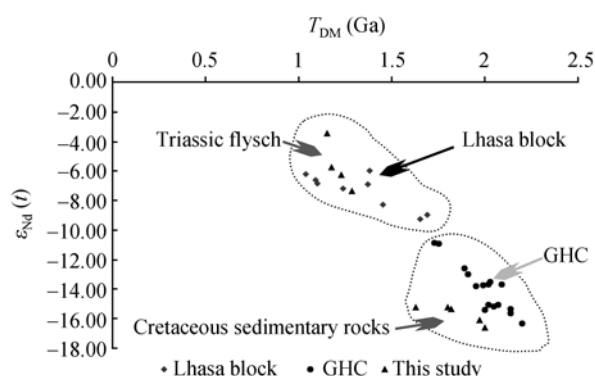


Figure 3 $\epsilon_{\text{Nd}}(t)$ vs. T_{DM} plot for samples from our study area and those from the High Himalayan Crystalline Complex in Bhutan^[8] and the Lhasa block^[34,64,65]. $\epsilon_{\text{Nd}}(t)$ values for two gneiss samples from the Nyaiqentanglha area are interpreted to represent middle and lower crust of the Lhasa terrane and are calculated at present time^[65]. $\epsilon_{\text{Nd}}(t)$ values for one granite gneiss sample and one gneissic granite from the Nyaiqentanglha area are calculated at 50 Ma according to their ages. $\epsilon_{\text{Nd}}(t)$ value for one granite sample derived from crust in the Bange area is calculated at 121 Ma. $\epsilon_{\text{Nd}}(t)$ values of two orthogneiss samples with their ages $>500 \text{ Ma}$ may represent the basement of the Lhasa terrane and two Early Permian shale samples from the northern Lhasa terrane are calculated at 210 Ma in order to compare with the Late Triassic flysch samples from this study^[34,64]. $\epsilon_{\text{Nd}}(t)$ values of schist and gneiss samples with their ages $>500 \text{ Ma}$ from Greater Himalayan complexes are calculated at 130 Ma. Two discrete fields can be identified. The Nd compositions of Late Triassic samples characterize the input of arc materials, as well as the Lhasa block. These observations are consistent with the results of Pan et al.^[66], which indicate that the Gangdese plutonic belt in the Lhasa terrane had experienced two phases of arc magmatism in the Late Triassic and Cretaceous to early Tertiary, respectively.

We note that more negative $\epsilon_{\text{Nd}}(0)$ values and older Nd model ages are associated with coarser-grained sedimentary samples than the finer-grained samples collected from the same sample locations (i.e., AY06-29-06-8A vs. AY06-29-06-8B; AY07-01-06-5B vs. AY07-01-06-5A; AY07-02-06-6A vs. AY07-02-06-6B) (Table 1). This observation may be explained by the coarser-grained components being mainly derived from continental sources associated with older crust and the finer-grained components being mainly derived from oceanic sources associated with younger crust.

4 Discussion and conclusions

The Nd compositions of our Late Triassic samples are drastically different from those of the Early Cretaceous samples (with the exception of sample AY07-02-06-4) in that the former have less negative $\epsilon_{\text{Nd}}(0)$ values and younger Nd model ages than the latter. The difference indicates that the two sequences were derived from very different sources; the protolith of the Triassic sediments was from a younger crust formed mostly at $\sim 1.15\text{--}1.29 \text{ Ga}$, whereas the protolith of the Cretaceous units were detritus from an older crust formed at $\sim 1.63\text{--}2.00 \text{ Ga}$. One possibility is that both units were derived from the Indian continent in the south, with the older Triassic rocks eroded from a younger crustal source at a shallower depth and the younger Cretaceous rocks from an older crustal source from a deeper crustal level. That is, the Nd compositions of the Triassic to Cretaceous strata essentially record an inverse stratigraphy of a crustal section with an increasing crustal-formation age downward. There are two problems with this interpretation. First, the existing Sm-Nd isotope data of the Late Triassic strata in southeast Tibet are similar to those obtained from the Lhasa terrane (Figure 3). Sedimentologic studies of the Triassic strata indicate that they were derived from a northern source, possibly the Lhasa block^[56]. In contrast, the Nd composition of the Cretaceous samples, with the exception of sample AY07-01-06-4, overlaps with the Nd composition of the GHC in Bhutan^[8] (Figure 3), suggesting a strong tie between the two Himalayan lithologic units. Based on these observations, we propose that the Triassic sediments were derived from the Lhasa block during its initial rifting from India as the Gondwana was breaking up (Figure 4). The rift valley must have been narrow enough to allow the submarine fan deposits to travel across the basin axis and to be de-

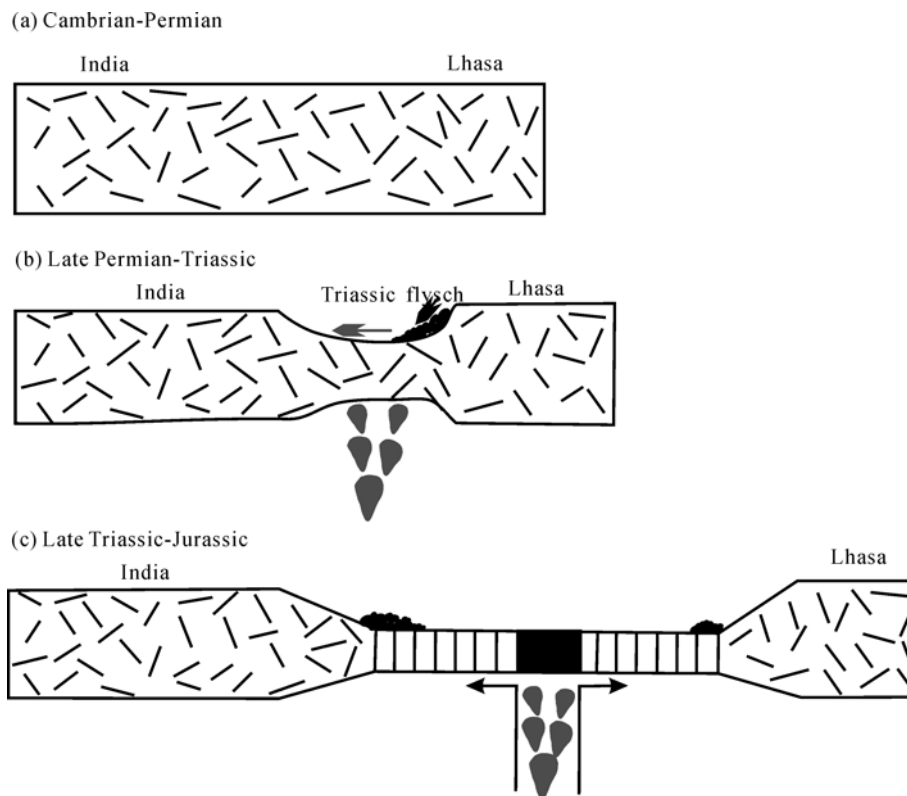


Figure 4 Schematic diagram showing a possible evolution of the Tethyan Himalaya from the Cambrian to the Jurassic. The continental rifting developed during the Late Permian to Early Triassic. The Late Triassic flysch sediments derived from the Lhasa block were transported and deposited on the future northern margin of Indian continent during the initial opening of the Tethyan ocean. Remnants of the Triassic sediments are preserved as part of the northern Indian passive margin sequence.

posited on the future northern margin of India. As the Lhasa block drifted away from India in the Jurassic, the Neo-Tethys was fully open causing isolation of sedimentation on the northern Indian margin from the Lhasa block^[15,16]. The Jurassic rifting may have been associated with the emplacement of mafic and ultramafic rocks in the southeastern Tibetan THS from 150 to 130 Ma^[67].

The above proposed model is quite preliminary and there are other possible explanations for the isotopic differences between the Triassic and Cretaceous strata and the southward flowing paleocurrent directions during deposition of the Triassic rocks. One possibility is that the Triassic strata were not part of the northern Indian passive margin sequence, but instead a mélangé complex jammed in the Indus-Tsangpo suture zone as envisioned by Yin^[4]. This explanation is possible as the highly deformed Late Triassic strata in southeast Tibet are commonly associated with ultramafic fragments whose ages and origins are poorly determined^[51]. The ultramafic rocks could be fragments of oceanic crust and thus parts of a large accretionary complex^[4]. From the

distribution of the ultramafic rocks, the southern boundary of the accretionary complex is the north-dipping northern thrust in the study area that juxtaposes Triassic and ultramafic rocks over the Jurassic-Cretaceous units, which have clear ties to the northern Indian margin sequence. In this alternative interpretation, the Late Triassic Langjiexue Group may have been deposited in a forearc setting at the onset of the subduction of the Neo-Tethys oceanic plate. The presence of Triassic volcanic rocks in the Lhasa block^[50,63] is consistent with this hypothesis. A problem with this interpretation is that the continuous subduction of the Tethyan oceanic plate would require a continuous development of a fore-arc basin from the late Triassic to the early Tertiary. The lack of Jurassic flysch complexes in our study does not support this prediction, although this could simply be an artifact of complete erosion of the Jurassic strata. Additionally, the Triassic volcanism in the Lhasa terrane could be completely related to subduction of the Bangong-Nujiang ocean from the north rather than a result of northward subduction of the Neo-Tethyan ocean from the south^[66]. Although we favor the interpretation that

the Triassic flysch deposits were derived from the Lhasa terrane at the initial breakup of the Gondwana supercontinent, we do not rule out the other possibilities such as an accretionary-prism origin for the Triassic flysch complex. Clearly, more detailed field mapping and a broader sampling scheme are required to better resolve the above issues.

We thank two anonymous reviewers for their constructive comments, which had led further clarification of the paper. We also thank Liang Xiaofeng and Peng Xiangdong for field assistance. We are grateful to Professors Li Xianghui, Chen Yuelong, Zhao Zhidan, and Zhang Yuxiu for discussion and their advice during the course of this study. Finally, we thank Professor Chen Fukun and Dr. Li Chaofeng for their assistance and guide in sample preparations and lab analysis. Dr. Tom Argles provided helpful comments on a preliminary draft of this manuscript.

- 1 Gansser A. The Geology of the Himalayas. New York: Wiley Interscience, 1964. 1–289
- 2 Burchfiel B C, Chen Z, Hodges K V, et al. The South Tibet Detachment System, Himalayan orogen: Extension contemporaneous with and parallel to shortening in a collisional mountain belt. Geological Society of America Special Paper, 1992, 269: 1–41
- 3 LeFort P. Evolution of the Himalaya. In: Yin A, Harrison T M, eds. The Tectonics of Asia. New York: Cambridge University Press, 1996. 95–106
- 4 Yin A. Cenozoic tectonic evolution of the Himalayan orogen as constrained by along-strike variation of structural geometry, exhumation history, and foreland sedimentation. Earth-Sci Rev, 2006, 76 (1-2): 1–131
- 5 LeFort P. Himalayas-collided range-present knowledge of continental arc. Am J Sci A, 1975, 275: 1–44
- 6 Brookfield M E. The Himalayan passive margin from Precambrian to Cretaceous. Sediment Geol, 1993, 84: 1–35
- 7 Gehrels G E, DeCelles P G, Martin A, et al. Initiation of the Himalayan Orogen as an early Paleozoic thin-skinned thrust belt. GSA Today, 2003, 13(9): 4–9
- 8 Richards A, Parrish R, Harris N, et al. Correlation of lithotectonic units across the eastern Himalaya, Bhutan. Geology, 2006, 34 (5): 341–344
- 9 Argles T W, Prince C I, Foster G L, et al. New Garnets for Old? Cautionary Tales from Young Mountain Belts. Earth Planet Sci Lett, 1999, 172: 301–309
- 10 Gehrels G E, DeCelles P G, Ojha T P, et al. Geologic and U-Pb geochronologic evidence for early Paleozoic tectonism in the Dadeldhura thrust sheet, far-west Nepal Himalaya. J Asian Earth Sci, 2006, 28(4-6): 385–408
- 11 Parrish R R, Hodges K V. Isotopic constraints on the age and provenance of the Lesser and Greater Himalayan Sequences, Nepalese Himalaya. Geol Soc Am Bull, 1996, 108: 904–911
- 12 DeCelles P G, Gehrels G E, Quade J, et al. Tectonic implications of U-PL zircon ages of the Himalayan orogenic belt in Nepal. Science, 2000, 288: 497–499
- 13 Myrow P M, Hughes N C, Paulsen T S, et al. Integrated tectonostratigraphic analysis of the Himalaya and implications for its tectonic reconstruction. Earth Planet Sci Lett, 2003, 212: 433–443
- 14 Garzanti E. Stratigraphy and sedimentary history of the Nepal Tethys Himalaya passive margin. J Asian Earth Sci, 1999, 17: 805–827
- 15 Liu G, Einsele G. Sedimentary history of the Tethyan basin in the Tibetan Himalayas. Geologische Rundschau, 1994, 82: 32–61
- 16 Liu G, Einsele G. Jurassic sedimentary facies and paleogeography of the former Indian passive margin in southern Tibet. In: Macfarlane A, Sorkhabi R B, Quade J, eds. Himalaya and Tibet: Mountain Roots to Mountain Tops. Geological Society of America Special Papers, 1999, 328: 75–108
- 17 Allègre C J, Courtillot V, Tapponnier P. Structure and evolution of the Himalayan-Tibet orogenic belt. Nature, 1984, 307: 17–22
- 18 Yin A, Harrison T M. Geologic evolution of the Himalayan-Tibetan orogen. Ann Rev Earth Planet Sci, 2000, 28: 211–280
- 19 Arita K. Origin of the inverted metamorphism of the Lower Himalayas Central Nepal. Tectonophysics, 1983, 95: 43–60
- 20 Godin L, Parrish R R, Brown R L, et al. Crustal thickening leading to exhumation of the Himalayan Metamorphic core of central Nepal: Insight from U-Pb geochronology and ⁴⁰Ar/³⁹Ar thermochronology. Tectonics, 2001, 20: 729–747
- 21 Searle M P, Godin L. The South Tibetan Detachment system and the Manaslu leucogranite: A structural re-interpretation and restoration of the Annapurna-Manaslu Himalaya, Nepal. J Geol, 2003, 111: 505–523
- 22 Martin A J, DeCelles P G, Gehrels G E, et al. Isotopic and structural constraints on the location of Main Central thrust in the Annapurna Range, central Nepal Himalaya. Geol Soc Am Bull, 2005, 117: 926–944
- 23 France-Lanord C, Derry L, Michard A. Evolution of the Himalaya since Miocene time: Isotopic and sedimentological evidence from the Bengal fan. In: Treloar P J, Searle P M, eds. Himalayan Tectonics. The Geological Society Special Publication, 1993, 74: 603–621
- 24 Najman Y, Garzanti E. Reconstructing early Himalayan tectonic evolution and paleogeography from Tertiary foreland basin sedimentary rocks, northern India. Geol Soc Am Bull, 2000, 112: 435–449
- 25 Ahmad T, Harris N, Bickle M, et al. Isotopic constraints on the structural relationships between the Lesser Himalayan Series and the High Himalayan Crystalline Series, Garhwal Himalaya. Geol Soc Am Bull, 2000, 112: 467–477
- 26 Robinson D M, DeCelles P G, Patchett P J, et al. The kinematic evolution of the Nepalese Himalaya interpreted from Nd isotopes. Earth Planet Sci Lett, 2001, 192: 507–521
- 27 Miller C, Thöni M, Frank W, et al. The early Palaeozoic magmatic event in the Northwest Himalaya, India: Source, tectonic setting and age of emplacement. Geol Mag, 2001, 138(3): 237–251
- 28 Richards A, Argles T, Harris N, et al. Himalayan architecture constrained by isotopic tracers from clastic sediments. Earth Planet Sci Lett, 2005, 236 (3-4): 773–796
- 29 Zhu D C, Pan G T, Mo X X, et al. Petrogenesis of volcanic rocks in the Sangxiu Formation, central segment of Tethyan Himalaya: A probable example of plume-lithosphere interaction. J Asian Earth Sci, 2007, 29 (2-3): 320–335
- 30 Deniel C, Vidal P, Fernandez A, et al. Isotopic study of the Manaslu granite (Himalaya, Nepal): Inferences on the age and source of the Himalayan leucogranites. Contrib Mineral Petrol, 1987, 96: 78–92
- 31 Inger S, Harris N. Geochemical constraints on leucogranite magmatism in the Langtang Valley, Nepal Himalaya. J Petrol, 1993, 34: 345–368

- 32 Whittington A, Foster G, Harris N, et al. Lithostratigraphic correlations in the western Himalaya — An isotopic approach. *Geology*, 1999, 27(7): 585—588
- 33 Walker R T, Nissen E, Molnar E, et al. Reinterpretation of the active faulting in central Mongolia. *Geology* 2007, 35: 759—762
- 34 Zhang K J, Zhang Y X, Li B, et al. Nd isotopes of siliciclastic rocks from Tibet, Western China: Constraints on provenance and pre-Cenozoic tectonic evolution. *Earth Planet Sci Lett*, 2007, 256(3-4): 604—616
- 35 Edwards M A, Kidd W S F, Li J X, et al. Multi-stage development of the southern Tibet detachment system near Khula Kangri. New data from Gonto La. *Tectonophysics*, 1996, 260: 1—19
- 36 Grujic D, Casey M, Davidson C, et al. Ductile extrusion of the Higher Himalayan Crystalline in Bhutan: Evidence from quartz microfabrics. *Tectonophysics*, 1996, 260: 21—43
- 37 Grujic D, Hollister L S, Parrish R R. Himalayan metamorphic sequence as an orogenic channel: Insight from Bhutan. *Earth Planet Sci Lett*, 2002, 198: 177—191
- 38 Grujic D, Coutand I B, Bookhagen S, et al. Climatic forcing of erosion, landscape, and tectonics in the Bhutan Himalayas. *Geology*, 2006, 34(10): 801—804
- 39 Gansser A. *Geology of the Bhutan Himalaya*. Boston: Birkhäuser Verlag, 1983. 1—180
- 40 Bhargava O N. *The Bhutan Himalaya: A geological account*. Geological Survey of India Special Publication, 1995, 39: 1—245
- 41 Daniel C G, Hollister L S, Parrish R R, et al. Exhumation of the Main Central Thrust from lower crustal depths, Eastern Bhutan Himalaya. *J Metamorph Geol*, 2003, 21: 317—334
- 42 Stüwe K, Foster D. $^{40}\text{Ar}/^{39}\text{Ar}$, pressure, temperature and fission-track constraints on the age and nature of metamorphism around the Main Central Thrust in the eastern Bhutan Himalaya. *J Asian Earth Sci*, 2001, 19: 85—95
- 43 Ding L, Zhong D L, Yin A, et al. Cenozoic structural and metamorphic evolution of the eastern Himalayan syntaxis (Namche Barwa). *Earth Planet Sci Lett*, 2001, 192: 423—438
- 44 Booth A L, Zeitler P K, Kidd W S F, et al. U-Pb zircon constraints on the tectonic evolution of southeastern Tibet, Namche Barwa area. *Am J Sci*, 2004, 304(10): 889—929
- 45 Zeitler P K, Meltzer A S, Koons P O, et al. Crustal reworking at Nanga Parbat, Pakistan: metamorphic consequences of thermal—mechanical coupling facilitated by erosion. *Tectonics*, 2001, 20: 712—728
- 46 Yin A, Harrison T M, Ryerson F J, et al. Tertiary structural evolution of the Gangdese thrust system, southeastern Tibet. *J Geophys Res*, 1994, 99: 18175—18201
- 47 Yin A, Harrison T M, Murphy M A, et al. Tertiary deformation history of southeastern and southwestern Tibet during the Indo-Asian collision. *Geol Soc Am Bull*, 1999, 111: 1644—1664
- 48 Ratschbacher L, Frisch W, Liu G, et al. Distributed deformation in southern and western Tibet during and after the India-Asia collision. *J Geophys Res*, 1994, 99: 19817—19945
- 49 Harrison T M, Yin A, Grove M, et al. The Zedong window: A record of superposed tertiary convergence in southeastern Tibet. *J Geophys Res*, 2000, 105: 19211—19230
- 50 Pan G T, Ding J, Yao D, et al. *Geological Map of Qinghai-Xiang (Tibet) Plateau and Adjacent Areas (1 : 1500000)*. Chengdu: Chengdu Cartographic Publishing House, 2004
- 51 Bureau of Geology and Mineral Resources of Xizang Region. *Regional Geology of Xizang (Tibet)*. Beijing: Geological Publish House, 1993
- 52 Xia J, Zhong H M, Tong J S, et al. Discovery of the ammonoid biota from the Lhakang Formation in southern Tibet and eastward extension of the northern Himalayan stratigraphic subprovince. *J Stratigr (in Chinese)*, 2005, 29(Supp): 579—581
- 53 Zhong H M, Xia J, Tong J S, et al. New results and major progress in regional geological survey of the Lhozag County Sheet. *Geol Bull Chin (in Chinese)*, 2004, 23(5-6): 451—457
- 54 Li X H, Zeng Q G, Wang C S. Palaeocurrent data: Evidence for the source of the Langjiexue Group in Southern Tibet. *Geol Rev (in Chinese)*, 2003, 49(2): 132—137
- 55 Li X H, Zeng Q G, Wang C S. Sedimentary characteristics of the upper Triassic Langjiexue Group in Southern Qingjie, Tibet. *Geoscience (in Chinese)*, 2003, 17(1): 52—58
- 56 Li X H, Zeng Q G, Wang C S. Provenance analysis of the upper Triassic Langjiexue Group in the Southern Tibet, China. *Acta Sediment Sin (in Chinese)*, 2004, 22(4): 553—559
- 57 Hegner E, Walter H J, Satir M. Pb-Sr-Nd isotopic compositions and trace element geochemistry of megacrysts and melilitites from the Tertiary Urach volcanic field: Source composition of small volume melts under SW Germany. *Contrib Mineral Petrol*, 1995, 122: 322—335
- 58 Chen F, Hegner E, Todt W. Zircon ages and Nd isotopic and chemical compositions of orthogneisses from the Black Forest, Germany: Evidence for a Cambrian magmatic arc. *Int J Earth Sci*, 2000, 88: 791—802
- 59 Chen F, Siebel W, Satir M, et al. Geochronology of the Karadere basement (NW Turkey) and implications for the geological evolution of the Istanbul zone. *Int J Earth Sci*, 2002, 91: 469—481
- 60 DePaolo D J. Neodymium isotopes in the Colorado Front Range and crust-mantle evolution in the Proterozoic. *Nature*, 1981, 291: 193—196
- 61 Liu Z Q. *Geologic Map of the Qinghai-Xizang Plateau and its Neighboring Regions (scale at 1:1500000)*. Chengdu Institute of Geology and Mineral Resources. Beijing: Geologic Publishing House, 1988
- 62 Baski A K, Barman T R, Paul D K, et al. Widespread early Cretaceous flood-basalt volcanism in eastern India—Geochemical data from the Rajmahal Bengal Sylhet traps. *Chem Geol*, 1987, 63: 133—141
- 63 LeFort P, Raŕ S M. Pre-Tertiary felsic magmatism of the Nepal Himalaya: recycling of continental crust. *J Asian Earth Sci*, 1999, 17: 607—628
- 64 Harris N B W, Xu R, Lewis C L, et al. Isotope geochemistry of the 1985 Tibet Geotraverse, Lhasa to Golmud. *Philos Trans R Soc London, Ser A*, 1988, 327: 263—285
- 65 King J, Harris N, Argles T, et al. First field evidence of southward ductile flow of Asian crust beneath southern Tibet. *Geology*, 2007, 35: 727—730
- 66 Pan G T, Mo X X, Hou Z Q, et al. Spatial-temporal framework of the Gangdese Orogenic Belt and its evolution. *Acta Petrol Sin*, 2006, 22(3): 521—533
- 67 Zhu D C, Mo X X, Pan G T, et al. Petrogenesis of the earliest Early Cretaceous mafic rocks from the Cona area of the eastern Tethyan Himalaya in south Tibet: Interaction between the incubating Kerguelen plume and the eastern Greater India lithosphere? *Litho*, 2008, 100: 147—173